scientific reports

Check for updates

OPEN

Development and validation of biopsy free nomograms for predicting clinically significant prostate cancer in men with PI-RADS 4 and 5 lesions

Junxin Wang[1,5], Mingzhe Chen[1,2,5], Shanqi Guo[3,5], Yong Xu[1], Liwei Liu[1]✉ & Xingkang Jiang[1,4]✉

To develop and validate biopsy-free nomograms to more accurately predict clinically significant prostate cancer (csPCa) in biopsy-naïve men with prostate imaging reporting and data system (PI-RADS) ≥ 4 lesions. A cohort of 931 patients with PI-RADS ≥ 4 lesions, undergoing prostate biopsies or radical prostatectomy from January 2020 to August 2023, was analyzed. Various clinical variables, including age, prostate-specific antigen (PSA) levels, prostate volume (PV), PSA density (PSAD), prostate health index (PHI), and maximum standardized uptake values (SUVmax) from PSMA PET-CT imaging, were assessed for predicting csPCa. Model performance was evaluated using area under the receiver operating characteristic curve (AUC), calibration plots, and decision-curve analyses, with internal validation. The foundational model (nomogram 1) encompassed the entire cohort, accurately predicting csPCa by incorporating variables such as age, PSAD, PV, PSA ratio variations, suspicious lesion location, and history of acute urinary retention (AUR). The AUC for csPCa prediction achieved by the foundational model was 0.918, with internal validation confirming reliability (AUC: 0.908). Advanced models (nomogram 2 and 3), incorporating PHI and PHI + PSMA SUVmax, achieved AUCs of 0.908 and 0.955 in the training set and 0.847 and 0.949 in the validation set, respectively. Decision analysis indicated enhanced biopsy outcome predictions with the advanced models. Nomogram 3 could potentially reduce biopsies by 92.41%, while missing only 1.53% of csPCa cases. In conclusion, the newly biopsy-free approaches for patients with PI-RADS ≥ 4 lesions represent a significant advancement in csPCa diagnosis in this high-risk population.

Keywords Magnetic resonance imaging, Nomograms, Prostate neoplasms, Positron emission tomography computed tomography, (18)F-PSMA-11

Prostate cancer (PCa) currently ranks as the most prevalent cancer and the second leading cause of cancer-related deaths among men, based on 2024 data[1]. Despite the widespread acceptance of prostate biopsy as the gold standard for diagnosis, it presents risks of physiological complications and psychological burdens, including urinary retention, hematuria, and sepsis, which can heighten preoperative anxiety[2,3]. Multiparametric magnetic resonance imaging (mpMRI) paired with the Prostate Imaging Reporting and Data System (PI-RADS) version 2.1 grading system has garnered significant attention in assessing the likelihood of clinically significant cancer. Elevated PI-RADS grades are linked to an increased likelihood of clinically significant prostate cancer (csPCa), sparking ongoing debates on the necessity of prostate biopsy, particularly for PI-RADS 4 and 5 grades.

[1]Department of Urology, The Second Hospital of Tianjin Medical University, No. 23 Pingjiang Road, Hexi Destrict, Tianjin 300211, China. [2]Department of Urology, Tianjin Medical University General Hospital, Tianjin 300052, China. [3]Department of Oncology, National Clinical Research Center for Chinese Medicine Acupuncture and Moxibustion, First Teaching Hospital of Tianjin University of Traditional Chinese Medicine, Tianjin 300381, China. [4]Tianjin Key Laboratory of Precision Medicine for Sex Hormones and Diseases (in Preparation), Tianjin 300211, China. [5] Junxin Wang, Mingzhe Chen and Shanqi Guo contributed equally to this work. ✉email: liuliwei3408@163.com; jiangx@tmu.edu.cn

While some advocate for bypassing biopsy entirely, others stress the importance of biopsy while minimizing unnecessary procedures[4–6].

While mpMRI accurately identifies csPCa, its low positive predictive value restricts its efficacy. Addressing this limitation, recent studies have introduced multivariable risk-based nomograms drawing on data from the European Randomized Study of Screening for PCa (ERSPC) and integrating mpMRI findings. This has resulted in enhanced cancer detection rates and a decrease in unnecessary biopsies[7–9]. Moreover, the incorporation of precision clinical parameters, such as the prostate health index (PHI) - comprising total PSA (tPSA), free PSA (fPSA), and the PSA isoform [-2]proPSA (p2PSA) - into a comprehensive formula has transformed csPCa screening practices. Meta-analyses have demonstrated that PHI exhibits superior sensitivity and specificity compared to traditional PSA markers for detecting csPCa, reaffirming its significance in screening guidelines[9,10]. Furthermore, molecular imaging techniques like prostate-specific membrane antigen (PSMA) positron emission tomography (PET)/computed tomography (CT) have been proposed for enhanced diagnostic accuracy in primary staging for PCa patients. Findings from the prospective PRIMARY trial have shown that combining PSMA PET with mpMRI surpasses the performance of mpMRI alone in detecting csPCa, indicating that men with suspicious PSMA-PET and mpMRI findings may potentially forego biopsy and proceed directly to definitive treatment[11,12]. However, to date, no studies have been conducted in highly suspicious patients incorporating both PHI and PSMA PET/CT images, along with multivariable clinical parameters, to predict the presence of csPCa.

Our study aims to investigate the potential development of biopsy-free diagnostic nomograms for csPCa in selected men with a high suspicion (PI-RADS ≥ 4) of significant malignancy in both PHI and PSMA PET/CT. The increasing interest in innovative imaging modalities for csPCa detection has prompted the creation and validation of biopsy-free nomograms based on a multivariate model incorporating clinical variables, PHI, and PSMA-PET/CT to estimate individual probabilities of aggressive PCa.

Methods

Study population

Data were retrospectively collected from two prospectively clinical studies (ChiCTR2200066455 and ChiCTR2000038696) conducted at the Second Hospital of Tianjin Medical University from January 2020 to August 2023. Biopsy-naïve patients suspected of having PCa due to elevated PSA and/or an abnormal DRE, along with highly suspicious lesions identified on the mpMRI (PI-RADS ≥ 4) were included. Exclusion criteria comprised: (1) Patients with urinary tract infection or prostatitis, (2) Patients who had undergone prostate surgery before biopsy, (3) Patients with incomplete clinical and pathological data, (4) Patients with poor MRI quality or low image resolution, and (5) Patients who had undergone previous prostate biopsies. The study was conducted in compliance with the guiding principles of the Declaration of Helsinki, and approved by the ethics committee of the Second Hospital of Tianjin Medical University (No.KY2020K130), and informed consent was obtained from each patient.

Collection of clinical information

The collected data for the whole population, and after stratification of the cohort according to the presence of csPCa includes the patients' age, height, weight, history of hypertension, history of diabetes, history of acute urinary retention (AUR) (within 1 month before biopsy), prostate volume (PV), last tPSA before biopsy, initial tPSA (within 1 month before biopsy), free PSA (fPSA), ratio of free PSA to total PSA (f/tPSA), PSA density (PSAD), digital rectal examination (DRE) findings, lesion localization on mpMRI, PI-RADS score, PHI (before biopsy), maximum standardized uptake value (SUVmax) on PSMA PET/CT, and pathological results. Calculation formulas for relevant clinical indicators are as follows: Body Mass Index (BMI): weight (kg) / height^2 (m^2), PSA differences to ratio: (last PSA before biopsy - initial PSA) / initial PSA * 100%. The serum concentration of total PSA, free PSA, and p2PSA was measured on the Access 2 analyzer (Beckman Coulter, Bream, CA, USA). The percentage of p2PSA (%p2PSA) was calculated using the formula [(p2PSA pg/ml)/(fPSA ug/L × 1000)] × 100. PHI was calculated using the formula: ([−2]proPSA/free PSA) × √PSA. PV was calculated using the formula PV = ([maximum anteroposterior diameter] × [maximum transverse diameter] × [maximum longitudinal diameter] × 0.52), as assessed through MRI imaging. PSAD was calculated by dividing total PSA by PV.

mpMRI protocol

We followed the European society of urogenital radiology (ESUR) guidelines and utilized a 3.0-T MRI protocol without endorectal coils for all participants. Two experienced genitourinary radiologists, each with over five years of experience in prostate MRI and blinded to patient clinical information, interpreted the scans according to the PI-RADS v2.1 protocol. This included multiparametric sequences: T2-weighted imaging (T2WI), diffusion-weighted imaging (DWI), and the calculation of apparent diffusion coefficient (ADC) maps using linear least squares regression. They independently assessed all MRI images, with PI-RADS scores of 4 and 5 indicating a high likelihood of csPCa.

PSMA PET-CT

All PSMA PET scans were conducted according to our local protocol and interpreted in a clinical setting. The recommended dosage range for 68Ga-PSMA-11 is typically 1.5-3.0 MBq/kg. However, the specific dosage for each patient is determined by the nuclear medicine physician based on their individual circumstances. After injection, there is a waiting period of usually 60 min to allow the tracer to distribute throughout the body and bind to PSMA. The patient lies on the scanning table, which gradually moves through the PET/CT machine. The entire process generally takes around 20–30 min. All PSMA PET scans are presented and discussed in a multidisciplinary meeting attended by at least two highly experienced nuclear medicine physicians. During the

analysis, several factors are considered, including PSMA uptake. Areas of high PSMA uptake may indicate the presence of prostate cancer. The uptake intensity and pattern, as well as the intensity of uptake, can provide insights into the nature of the cancer. Uptake in other areas, such as lymph nodes or other organs, may suggest the spread of cancer. Standardized uptake values (SUV) are typically used to quantify PSMA uptake.

Histopathological analysis

Enrolled patients were underwent either ultrasound-guided transperineal prostate biopsy (combined systematic and targeted biopsy) or radical prostatectomy. Tissue samples were fixed in formalin and evaluated by two senior pathologists specializing in prostate evaluation, adhering to 2019 International Society of Urological Pathology standards. csPCa was defined as those with a Gleason score of $\geq 3+4$, while non-csPCa was defined by the absence of csPCa and included cases of benign prostatic hyperplasia, prostatitis, prostatic hyperplasia, and normal prostate tissue with calcification.

Statistical analyses

The statistical analyses were performed using statistical package for social science version 22.0 (SPSS 22.0, IBM Corp) and R version 4.3.2 (www.r-project.org). Descriptive statistics were used to summarize continuous variables, which were compared between the diagnostic and validation cohorts using the Wilcoxon rank-sum and Kruskal-Wallis tests. Categorical variables were presented as frequencies (percentages), and group comparisons were conducted using the chi-square test or Fisher's exact test. Multiple imputation was utilized for variables with missing or outlier values, with the normality of continuous variables assessed using the Shapiro-Wilk test. Disaggregated data were presented as numbers (n) and percentages (%). Normally distributed continuous variables were expressed as mean ± standard deviation (SD), while non-normally distributed ones were described as the median (interquartile range (IQR)). The cut-off value of the nomogram was determined using the maximum Youden index, with a significance level set at $p<0.05$. The entire cohort was randomly divided into a training cohort and a validation cohort at a 7:3 ratio. Univariate logistic regression analysis was initially conducted in the modeling dataset, followed by backward multiple logistic regression analysis after excluding variables exhibiting multicollinearity. Variables with $p<0.05$ were retained for model establishment. The prediction model was developed using a nomogram and internally validated to assess its predictive performance. The area under the receiver operating characteristic (ROC) curve (AUC) was calculated to evaluate discrimination ability, with model calibration assessed using the Hosmer-Lemeshow test and calibration curve. Decision curve analysis (DCA) evaluated net benefit and clinical utility.

Results

Clinical characteristics

A total of 931 patients met the inclusion criteria and were included in the overall population (Fig. 1). The baseline characteristics of the patients are presented in (Table 1). Among them, 779 (83.7%) patients received a diagnosis of csPCa and 152 (16.3%) patients were diagnosed with non-csPCa. Patients with csPCa exhibited higher levels of age, PSA, fPSA, PSAD, percentage differences in PSA ratio, PI-RADS score, peripheral zone location, acute urinary retention, diabetes, DRE findings, and lower PV and %f/TPSA compared to those with non-csPCa. In the cohort of 316 and 198 patients undergoing PHI and PSMA PET/CT imaging, the PHI and PSMA SUVmax were notably elevated in individuals with csPCa compared to those with non-csPCa (Tables S1, S2). Among these patients, a random assignment of 7:3 was made to the training and validation cohorts, and a detailed comparison of demographic data, comorbidities, and characteristics between the three cohorts is presented in (Tables S3–S6).

Prediction model development

After multivariate analysis, factors including age, PV, PSAD, and %PSA differences to ratio, peripheral zone location, and AUC were identified as strong associated with csPCa findings within the whole cohort (Table 2, Table S7). Subsequently, the foundational nomogram (model 1) comprised of age, PV, PSAD, %PSA differences to ratio, localization of suspicious lesion, and AUC, demonstrated an AUC of 0.918 (95% confidence interval [CI] 0.894–0.943) following internal validation. Additionally, when integrating PHI into the baseline model, age and %PSA differences to ratio were excluded from nomogram 2, resulting in an AUC of 0.908 (95% CI 0.863–0.953). The incorporation of PHI and PSMA SUVmax into the foundational nomograms (model 3), which included PHI, PSMA SUVmax, localization of suspicious lesion, and AUR, led to a substantial enhancement in the AUC for predicting csPCa, elevating it to 0.955 (95% CI 0.923–0.987) (Figs. 2, 3).

Decision curve analysis

The calibration plot demonstrates superior fit of the advanced model compared with the baseline model in both the training cohort and validation cohort (Figure S1). To validate the efficacy of the nomogram, a decision curve analysis (DCA) was conducted, revealing that advanced models enhanced clinical risk prediction for csPCa with a threshold probability of 80%, with models 2 and 3 graphically superior to model 1 (38.78 vs. 51.86 and 53.57) (Figure S2). For the optimal cutoff values of PSAD, PHI, SUVmax, and nomograms in predicting csPCa in these highly suspicious patients with PI-RADS 4 and 5 lesions, a comprehensive analysis of various thresholds was conducted, and the findings are summarized in (Table 3). Using a cutoff of 38.9%, the proportion of patients eligible for biopsy-free was 92.41%, at the cost of missing 1.53% patients with csPCa.

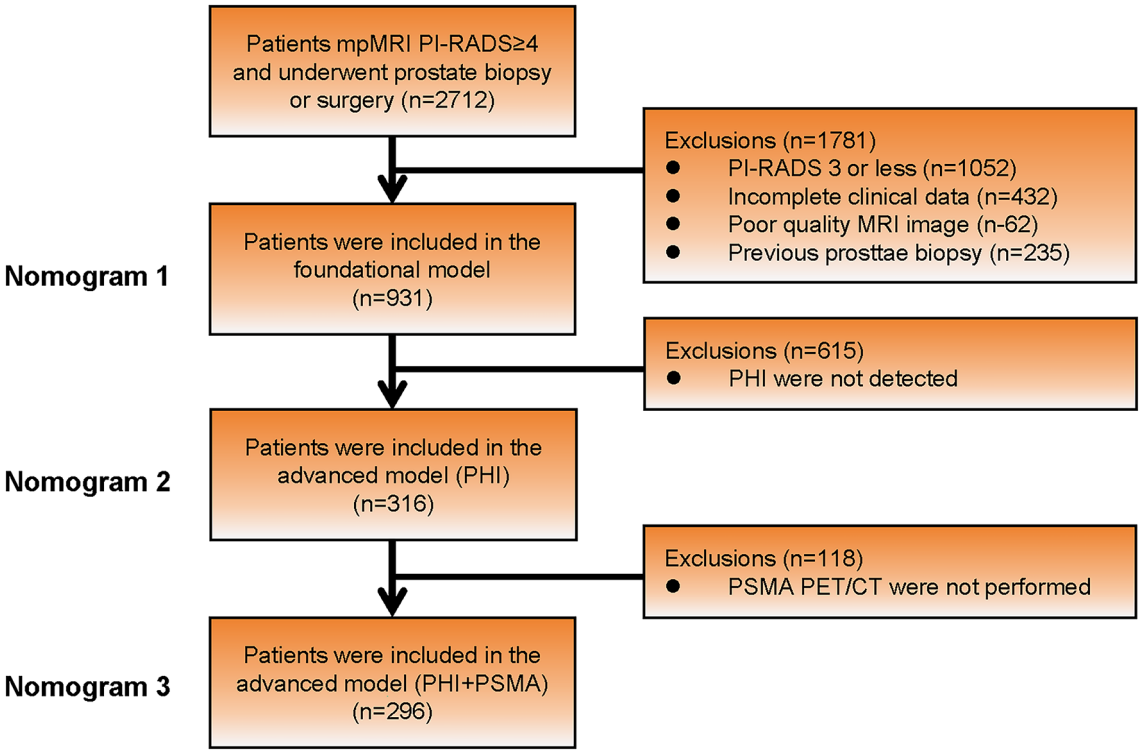

Fig. 1. Consolidated standards of reporting trials (CONSORT) diagram illustrating the inclusion of patients in the whole cohorts.

Discussion

Many nomograms target the "gray zone" of PSA levels (4–20 ng/mL) or PI-RADS score 3, aiming to identify patients unlikely to have prostate cancer and avoid unnecessary biopsies[8–10]. Our study focuses on the high-risk group with PI-RADS scores of 4 or higher to accurately detect prostate cancer and minimize unnecessary biopsies. In 2020, a comprehensive cross-sectional study unveiled that PI-RADS scores of 4 and 5 are robust indicators of a high suspicion of csPCa, with corresponding positive predictive values of 39 and 72%[13]. By 2023, Xiang et al. developed a predictive model based on patient-related characteristics for the detection of PCa in individuals with PI-RADS 4–5 lesions. Their study, which involved 833 patients, demonstrated that 83.0% of prostate cancer cases were identified in those with PI-RADS scores of 4 or higher, with 74.5% in PI-RADS 4 lesions and 91.8% in PI-RADS 5 lesions. Notably, independent characteristics within the PI-RADS 4 subgroup, such as lesion location, age, fPSA/total PSA ratio, and PSAD, were identified and used to establish the predictive model, achieving an AUC of 0.748 (95% CI 0.694–0.803). Additionally, the prediction model for PI-RADS 5 was developed based on PSA and PSAD, resulting in an AUC of 0.893 (95% CI 0.844–0.941)[14]. In the present study involving 981 patients, the diagnostic rate of csPCa was 83.7%, with 67.1% identified in PI-RADS 4 lesions and 94.8% in PI-RADS 5 lesions. Our study established and validated a fundamental diagnostic nomogram that obviates the need for biopsy in predicting csPCa, achieving an AUC of 0.918 (95% CI 0.894–0.943). This nomogram incorporates preclinical parameters such as age, PV, PSAD, suspicious lesion location, and %PSA differences to ratio, and AUR. While our results reinforce the connection between higher PI-RADS scores and an increased likelihood of csPCa, a small subset of individuals still received negative biopsy results, highlighting the hesitance to avoid prostate biopsies. Factors contributing to "false-positive MRI diagnoses" include PI-RADS overestimation, ambiguous images leading to inflated PI-RADS scores, diseases posing challenges in differentiation, and missed lesions during initial biopsies, with the former two factors being predominant[15–17]. Given these considerations, integrating additional clinical parameters and molecular imaging may be essential to enhance multiparametric MRI interpretations for accurate csPCa prediction and potentially reduce the necessity for unnecessary prostate biopsies in individuals with highly suspicious PI-RADS ≥ 4 lesions.

Several studies have indicated that integrating PHI into multivariate models comprising clinical and demographic variables enhances diagnostic accuracy in predicting csPCa. For instance, Zhou et al.[18] showed that the combined assessment of PHI, PI-RADS scores, and other clinical factors (such as age, PI-RADS, and Log PSA Density) yielded AUC values of 0.902 for PCa and 0.896 for csPCa, respectively. Similarly, Mo et al.[19] presented a multivariable model incorporating PI-RADS, fPSA, PHI, we evaluated the diagnostic precision of PHI and apparent diffusion coefficient (ADC) values based on PI-RADS v2.1 for guiding prostate biopsy in patients with PSA levels ranging from 4 to 20 ng/mL. The predictive model we devised, comprising age, PHI, PV, and ADC values as independent predictors, demonstrated an AUC of 0.856 for predicting csPCa[10]. In the current work, we also validated that PHI improves the detection rate of csPCa in patients with PI-RADS ≥ 4 lesions, in line with previous findings. Incorporating PHI into the basic variables, Model 2 demonstrated a comparable AUC

	Whole cohort ($n=931$)	Non-csPCa ($n=152$)	csPCa ($n=779$)	p value
Age at biopsy (yr), median (IQR)	71 (66–76)	69 (65.00-73.75)	71 (66–76)	**<0.001**
BMI (kg/m2), median (IQR)	24.45 (22.49–26.45)	24.25 (22.49–26.83)	24.45 (22.49–26.42)	0.865
PSA (ng/ml), median (IQR)	31.90 (12.30-78.58)	10.25 (6.11–20.48)	42.33 (16.53–87.58)	**<0.001**
PSA, n (%)				**<0.001**
≤4	19 (2.04)	14 (9.21)	5 (0.64)	
4–20	319 (34.26)	100 (65.79)	219 (28.11)	
20–50	243 (26.10)	32 (21.05)	211 (27.09)	
>50	350 (37.60)	6 (3.95)	344 (44.16)	
fPSA (ng/ml), median (IQR)	3.49 (1.51–8.82)	1.71 (0.86–2.81)	4.49 (1.75-10.00)	**<0.001**
% f/tPSA, median (IQR)	10.95 (8.23–15.19)	14.03 (9.26–20.81)	10.61 (8.13–14.16)	**<0.001**
Testosterone (ng/dl), median (IQR)	377.62 (299.80-449.57)	385.74 (330.90-452.86)	374.76 (297.12-449.25)	0.244
PV (ml), median (IQR)	55.09 (37.61–75.79)	65.10 (49.22–96.78)	53.20 (36.36–72.80)	**<0.001**
PV, n (%)				**<0.001**
≤50	397 (42.64)	40 (26.32)	357 (45.83)	
>50	534 (57.36)	112 (73.68)	422 (54.17)	
PSAD (ng/ml2), median (IQR)	0.62 (0.25–1.28)	0.17 (0.10–0.29)	0.78 (0.37–1.45)	**<0.001**
PSAD, n (%)				**<0.001**
≤0.2	187 (20.09)	91 (59.87)	96 (12.32)	
0.2–0.5	208 (22.34)	44 (28.95)	164 (21.05)	
0.5–1.0	227 (24.38)	16 (10.53)	211 (27.09)	
>1.0	309 (33.19)	1 (0.65)	308 (39.54)	
%PSA differences to ratio, median (IQR)	−0.33 (−16.32–10.15)	−21.93 (−40.94–2.70)	1.84 (−9.84–12.12)	**<0.001**
%PSA differences to ratio, n (%)				**<0.001**
≤−50	51 (5.48)	34 (22.37)	17 (2.18)	
−50–20	133 (14.29)	44 (28.95)	89 (11.42)	
>−20	747 (80.23)	74 (48.68)	673 (86.40)	
PI-RADS score, n (%)				**<0.001**
4	374 (40.17)	123 (80.92)	251 (32.22)	
5	557 (59.83)	29 (19.08)	528 (67.78)	
Localization of suspicious lesion, n (%)				**<0.001**
PZ	466 (50.05)	81 (53.29)	385 (49.42)	
TZ	124 (13.32)	46 (30.26)	78 (10.01)	
Others	61 (6.55)	23 (15.13)	38 (4.88)	
PZ + TZ	280 (30.08)	2 (1.32)	278 (35.69)	
AUR, n (%)	144 (15.47)	45 (29.61)	99 (12.71)	**<0.001**
Diabetes, n (%)	197 (21.16)	22 (14.47)	175 (22.46)	**0.027**
Hypertension, n (%)	412 (44.25)	70 (46.05)	342 (43.90)	0.625
DRE, n (%)	521 (55.96)	66 (43.42)	455 (58.41)	**0.001**

Table 1. Patients' characteristics of enrolled population ($n=931$). *BMI* body mass index, *IQR* inter quartile range, *PI-RADS* prostate imaging reporting and data system, *PSA* prostate-specific antigen, *PSAD* prostate-specific antigen density, *PZ* peripheral zone, *TZ* transition zone, *Others* lesions beyond the peripheral and transition zones, *DRE* digital rectal examination. The p values were calculated using the chi-square (categorical variables) and Mann-Whitney (continuous variables) tests. p-values < 0.05 in bold.

to Model 1 in both the training and validation cohorts (AUC: 0.918 vs. 0.908, and 0.908 vs. 0.847, respectively). The observed similarity in AUC between Model 1 and Model 2 may be attributed to the relatively small sample size. With a smaller sample size, the statistical power to detect differences between models might be diminished. Additionally, we utilized the entire cohort of 316 patients for training and consistently obtained similar results during nomogram validation. Consequently, even if Model 2 exhibits improvement over Model 1, it might not achieve statistical significance due to the limitations imposed by the sample size. Therefore, a larger sample size might be necessary to more accurately assess the performance differences between these models.

The advanced molecular imaging technique, PSMA PET/CT, offers superior diagnostic precision in identifying various conditions of PCa, including active surveillance, biochemical recurrence, lymph node metastasis, as well as metastatic castration-resistant disease, potentially influencing treatment decisions[20]. Therefore, incorporating PSMA PET/CT into screening programs as an adjunctive tool can assist in decreasing the overdiagnosis of insignificant cancer, while also enhancing the diagnostic accuracy for csPCa[21–23]. Despite cost considerations, several authors have recommended the use of PSMA PET/CT due to potential cost savings and improved

	Model 1		Model 2		Model 3	
	OR (95% CI)	*p* value	OR (95% CI)	*p* value	OR (95% CI)	*p* value
Age	1.07 (1.02–1.11)	**0.003**	–	–	–	–
PV			0.98 (0.97–1.00)	**0.014**	–	–
≤ 50	Reference group					
> 50	0.38 (0.21–0.70)	**0.002**				
PSAD			3.65 (0.48–28.02)	0.213	–	–
≤ 0.2	Reference group					
0.2–0.5	2.67 (1.43–4.99)	**0.002**				
0.5–1.0	5.73 (2.64–12.42)	**< 0.001**				
> 1.0		0.977				
%PSA differences to ratio			–	–	–	–
≤ −50	Reference group					
−50–20	4.32 (1.35–13.86)	**0.014**				
> −20	7.27 (2.46–21.44)	**< 0.001**				
PHI, median	–	–	1.02 (1.01–1.03)	**0.001**	1.01 (1.00–1.02)	**0.047**
PSMA PET/CT SUV max	–	–	–	-	1.25 (1.06–1.47)	**0.009**
Localization of suspicious lesion						
PZ	Reference group		Reference group		Reference group	
TZ	0.28 (0.15–0.54)	**< 0.001**	0.17 (0.05–0.52)	**0.002**	0.08 (0.02–0.46)	**0.004**
Others	0.31 (0.12–0.82)	**0.018**	0.24 (0.05–1.09)	**0.065**	1.28 (0.10–16.93)	0.851
PZ + TZ	18.50 (2.35–145.4)	**0.006**	2.50 (0.28–22.07)	0.411	6.26 (0.53–74.45)	0.146
AUR						
None	Reference group		Reference group		Reference group	
Yes	0.25 (0.11–0.57)	**0.001**	0.21 (0.02–0.71)	**0.012**	0.10 (0.02–0.54)	**0.007**

Table 2. Multivariable logistic regression analysis for predicting clinically significant prostate cancer (csPCa) using three models. *csPCa* clinically significant prostate cancer, *OR* odds ratio, *CI* confidence interval, *AIC* akaike information criterion, *PHI* prostate health index, *PET* positron emission tomography, *PI-RADS* prostate imaging reporting and data system, *PSAD* prostate-specific antigen density, *PSMA* prostate-specific membrane antigen, *PZ* peripheral zone, *TZ* transition zone, *Others* lesions beyond the peripheral and transition zones. a AIC min = 344.82. b AIC min = 142.28. c AIC min = 71.13.

quality of life resulting from avoid unnecessary biopsies. By employing preclinical risk stratification with PSMA-PET/CT imaging, some individuals have successfully undergone radical prostatectomy without prior biopsy, presenting promising outcomes and potentially eliminating the need for biopsy in patients with highly suspicious lesions rated PI-RADS ≥ 4[5,24–27]. However, as the saying goes, "all truth passes through three stages: first, it is ridiculed; second, it is violently opposed; third, it is accepted as self-evident." Considering this context, our objective was to investigate the feasibility and outcomes of a biopsy-free approach based on preclinical risk stratification, integrating PHI and PSMA SUVmax in patients with highly suspicious lesions rated PI-RADS ≥ 4. By incorporating both PHI and PSMA SUVmax, the model 3 exhibited superior discriminatory power compared to the foundational nomogram (model 1) and model 2 (AUC: from 0.918 to 0.908 to 0.955). Additionally, model 3 exhibited outstanding calibration in predicting the risk of csPCa, suggesting that incorporation of this advanced model into clinical practice could potentially eliminate the need for prostate biopsy.

While our study possesses notable strengths, it is imperative to acknowledge its limitations. First, the retrospective nature of our analysis may introduce patient selection biases, potentially affecting the generalizability of our findings. Second, our study focused on patients with PI-RADS ≥ 4 lesions at a single institution, where mpMRIs and PSMA PET/CT were predominantly interpreted by experienced radiologists. This may limit the applicability of our findings to institutions with less experienced radiologists. Additionally, variations in PSMA tracers can influence SUVmax values, underscoring the need for future research in diverse settings. Third, the relatively small number of patients, especially those who underwent both PHI and PSMA PET/CT imaging, may introduce selection bias. This is particularly notable due to the high proportion of patients with PSA > 20 ng/mL. We also acknowledge the 16.46% of patients with recent urinary retention, which may impact selection bias and align with real-world scenarios. Furthermore, we did not conduct external validation for our novel nomogram, a crucial step before clinical application to ensure its reliability and generalizability across different patient populations. Fourth, our study included patients with PI-RADS ≥ 4 and confirmed pathological diagnoses, obtained either through biopsies or RP. Of these, 82 patients underwent RP without prior biopsy, providing complete preoperative clinical data (PSA, PV, MRI) and pathological results (ISUP), ensuring the reliability of the data and the nomogram. The remaining patients were diagnosed via biopsies. However, since the pathological findings are based solely on biopsy results without RP, they may underestimate the actual tumor burden. Therefore, interpreting our results requires consideration of the biopsy methods and their limitations. Notably, followed up of biopsy-negative patients revealed no newly positive cases. Finally, these nomograms are designed to provide

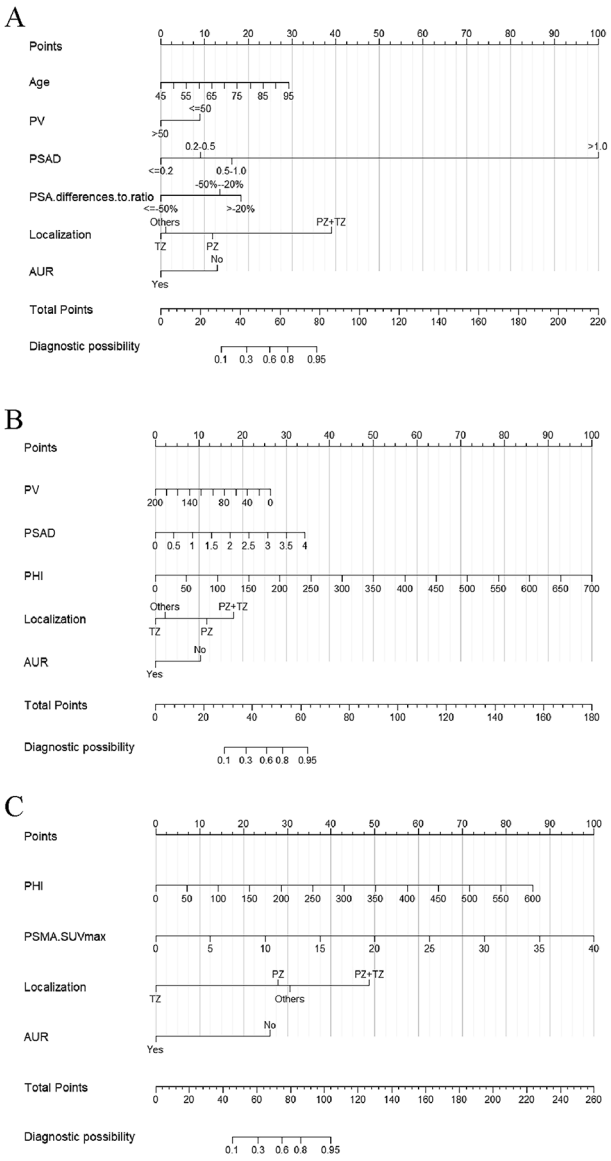

Fig. 2. Three Nomograms for predicting clinically significant prostate cancer. (**A**) Nomogram 1 (fundamental nomogram) featuring multivariable preclinical parameters. (**B**) Nomogram 2, incorporating the combination of PHI with basic parameters. (**C**) Nomogram 3, incorporating PHI, PMSA SUVmax, and basic parameters.

clinicians with a quantitative tool to support decision-making in avoiding unnecessary biopsies. They are not intended as simple binary tools but as nuanced approaches to guide clinical judgment. The time, cost, and resource implications of using PHI and PSMA PET/CT must also be considered when evaluating their benefits in a biopsy-free strategy. For patients with negative MRI results, additional diagnostic tools are still necessary for differential diagnosis. Our model complements MRI findings, offering a comprehensive approach to identifying clinically significant prostate cancers.

Conclusions

Our study developed a novel multivariate biopsy-free nomogram that incorporates PHI and PSMA SUVmax data, aiming to avoid unnecessary prostate biopsies in patients with PI-RADS≥4 lesions. This nomogram enhances preoperative counseling, helping clinicians make well-informed decisions about prostate biopsies. However, further prospective studies are essential to validate its efficacy and reliability.

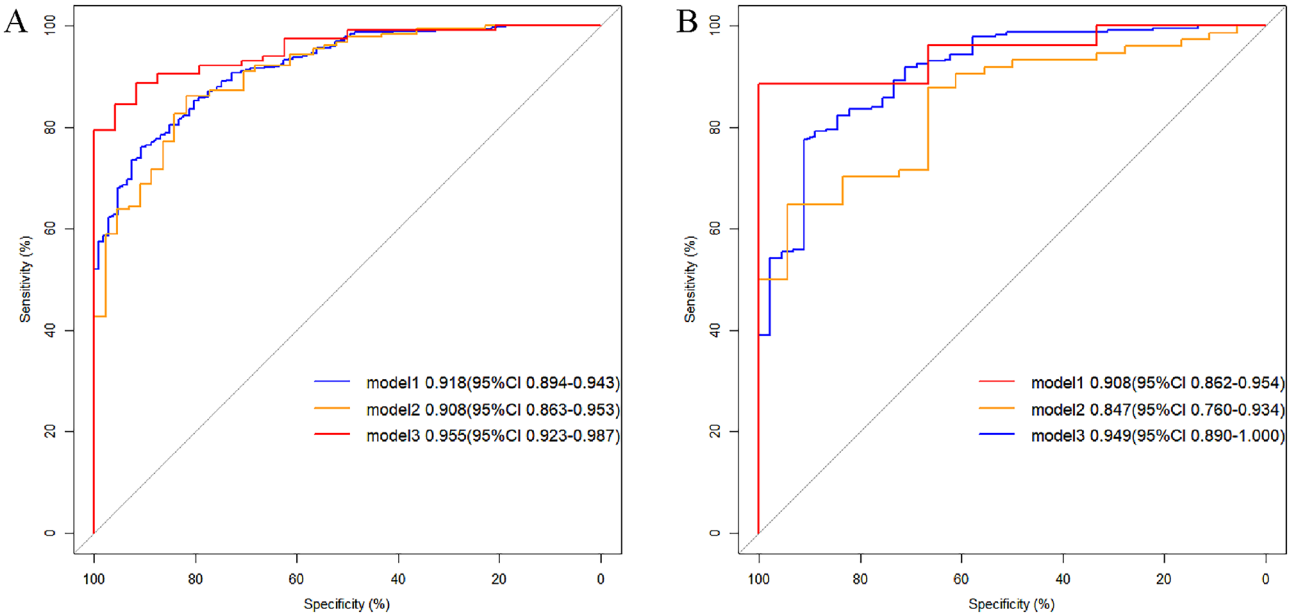

Fig. 3. The receiver operating characteristic (ROC) curve of (**A**) training cohort and (**B**) validation cohort for highly suspected prostate cancer (PI-RADS ≥ 4 lesions). Model 1 includes age, PV, PSAD, PSA differences to ratio, localization, and AUR. Model 2 includes PV, PSAD, PHI, localization, and AUR. Model 3 includes PHI, PSMA SUVmax, localization, and AUR.

	Decision to biopsy	sensitivity, %	Specificity, %	PPV, %	NPV, %	%Avoided biopsy	%Missed CsPCa
n = 931	NP[a] ≥ 0.757	87.16	79.61	95.63	54.82	85.96	10.71
	NP[b] ≥ 0.458	98.10	51.30	91.17	84.05	90.46	1.59
	NP[c] ≥ 0.991	46.10	100.00	100.00	26.58	54.90	45.10
n = 316	NP[a] ≥ 0.852	77.20	83.90	95.16	47.32	78.51	18.33
	NP[b] ≥ 0.389	96.50	53.20	89.42	78.77	88.00	2.81
	NP[c] ≥ 0.987	37.00	100.00	100.00	27.93	49.36	50.00
	PHI[a] ≥ 94.570	68.90	88.90	96.22	41.10	72.82	25.00
	PHI[b] ≥ 45.59	95.50	50.00	88.71	74.85	86.89	3.30
	PHI[c] ≥ 203.160	32.40	100.00	100.00	23.53	45.66	54.34
	PSAD[a] ≥ 9.480	78.40	61.10	89.20	40.84	75.01	17.36
	PSAD[b] ≥ 4.545	89.20	44.40	86.79	50.09	80.41	8.68
	PSAD[c] ≥ 1.640	14.90	100.00	100.00	22.29	31.60	68.40
n = 198	NP[a] ≥ 0.852	86.31	93.33	98.63	54.88	87.36	11.62
	NP[b] ≥ 0.389	98.20	60.00	93.22	85.62	92.41	1.53
	NP[c] ≥ 0.954	72.60	100.00	100.00	39.46	76.75	23.25
	PHI[a] ≥ 94.570	79.17	83.33	96.37	41.70	79.82	17.65
	PHI[b] ≥ 45.59	97.60	43.30	90.60	76.31	89.37	2.04
	PHI[c] ≥ 200.715	46.50	100.00	100.00	24.99	54.52	45.48
	PSMA SUV max[a] ≥ 9.480	78.57	76.67	94.97	39.03	78.31	18.16
	PSMA SUV max[b] ≥ 4.545	97.00	36.70	89.56	68.60	87.86	2.55
	PSMA SUV max[c] ≥ 16.520	45.80	100.00	100.00	24.78	54.01	45.99

Table 3. Predictive performance of different cut-off values of prostate-specific antigen density (PSAD), prostate health index (PHI), maximum standardized uptake value (SUVmax), and three nomograms. *csPCa* clinically significant prostate cancer, *PI-RADS* prostate imaging reporting and data system, *NP* nomogram predictive, *NPV* negative predictive value, *PHI* prostate health index, *PPV* positive predictive value, *PSAD* prostate-specific antigen density, *PET* positron emission tomography, *PSMA* prostate-specific membrane antigen. [a]The cut-off value at the maximum Youden index. [b]The cut-off value at maximum accuracy. [c]The cut-off value at maximum specificity.

Data availability

The data are available from the corresponding author upon reasonable request.

Received: 6 July 2024; Accepted: 13 January 2025
Published online: 20 January 2025

References

1. Siegel, R. L. et al. Cancer statistics. *CA Cancer J. Clin.* **74** (1), 12–49. https://doi.org/10.3322/caac.21820 (2024).
2. Connor, M. J. et al. Landmarks in the evolution of prostate biopsy. *Nat. Rev. Urol.* **20** (4), 241–258. https://doi.org/10.1038/s41585-022-00684-0 (2023).
3. Vanoli, S. et al. Evolution of anxiety management in prostate biopsy under local anesthesia: a narrative review. *World J. Urol.* **42** (1), 43. https://doi.org/10.1007/s00345-023-04723-2 (2024).
4. Meissner, V. H. et al. Radical prostatectomy without prior biopsy following multiparametric magnetic resonance imaging and prostate-specific membrane antigen positron emission tomography. *Eur. Urol.* **82** (2), 156–160. https://doi.org/10.1016/j.eururo.2021.11.019 (2022).
5. Modi, P. K. et al. Radical prostatectomy without biopsy: audacious, imprudent, or innovative? *Eur. Urol.* **82** (2), 161–162. https://doi.org/10.1016/j.eururo.2022.03.008 (2022).
6. Turkbey, B. et al. PI-RADS: where next? *Radiology* **307** (5), e223128. https://doi.org/10.1148/radiol.223128 (2023).
7. Remmers, S. et al. Reducing biopsies and magnetic resonance imaging scans during the diagnostic pathway of prostate cancer: applying the rotterdam prostate cancer risk calculator to the PRECISION trial data. *Eur. Urol. Open. Sci.* **36**, 1–8 (2021).
8. Siddiqui, M. R. et al. Optimizing detection of clinically significant prostate cancer through nomograms incorporating mri, clinical features, and advanced serum biomarkers in biopsy naïve men. *Prostate Cancer Prostat. Dis.* **26** (3), 588–595. https://doi.org/10.1038/s41391-023-00660-8 (2023).
9. Chung, J. H. et al. Nomogram using prostate health index for predicting prostate cancer in the gray zone: prospective, multicenter study. *World J. Mens Health* **42** (1), 168–177. https://doi.org/10.5534/wjmh.220223 (2024).
10. Huang, H. et al. Based on PI-RADS v2.1 combining PHI and ADC values to guide prostate biopsy in patients with PSA 4–20 ng/mL. *Prostate* **84** (4), 376–388. https://doi.org/10.1002/pros.24658 (2024).
11. Emmett, L. et al. The PRIMARY score: using intraprostatic 68Ga-PSMA PET/CT patterns to optimize prostate cancer diagnosis. *J. Nucl. Med.* **63** (11), 1644–1650. https://doi.org/10.2967/jnumed.121.263448 (2022).
12. Kelly, B. D. et al. A novel risk calculator incorporating clinical parameters, multiparametric magnetic resonance imaging, and prostate-specific membrane antigen positron emission tomography for prostate cancer risk stratification before transperineal prostate biopsy. *Eur. Urol. Open. Sci.* **53**, 90–97. https://doi.org/10.1016/j.euros.2023.05.002 (2023).
13. Westphalen, A. C. et al. Variability of the positive predictive value of PI-RADS for prostate MRI across 26 centers: experience of the society of abdominal radiology prostate cancer disease-focused panel. *Radiology* **296** (1), 76–84. https://doi.org/10.1148/radiol.2020190646 (2020).
14. Xiang, L. et al. Patient-related characteristics predict prostate cancers in men with PI-RADS 4–5 to further optimize the diagnostic performance of MRI. *Abdom. Radiol.* **48** (12), 3766–3773. https://doi.org/10.1007/s00261-023-04011-y (2023).
15. Wang, Y. H. et al. Improving the understanding of PI-RADS in practice: characters of PI-RADS 4 and 5 lesions with negative biopsy. *Asian J. Androl.* **25** (2), 217–222. https://doi.org/10.4103/aja2022112 (2023).
16. Stavrinides, V. et al. Regional histopathology and prostate MRI positivity: a secondary analysis of the PROMIS trial. *Radiology* **307** (1), e220762. https://doi.org/10.1148/radiol.220762 (2023).
17. Norris, J. M. et al. What type of prostate cancer is systematically overlooked by multiparametric magnetic resonance imaging? An analysis from the PROMIS cohort. *Eur. Urol.* **78** (2), 163–170. https://doi.org/10.1016/j.eururo.2020.04.029 (2020).
18. Zhou, Y. et al. Nomograms combining PHI and PI-RADS in detecting prostate cancer: a multicenter prospective study. *J. Clin. Med.* **12** (1), 339. https://doi.org/10.3390/jcm12010339 (2023).
19. Mo, L. C. et al. Development of a novel nomogram for predicting clinically significant prostate cancer with the prostate health index and multiparametric MRI. *Front. Oncol.* **12**, 1068893. https://doi.org/10.3389/fonc.2022.1068893 (2022).
20. Caracciolo, M. et al. PSMA PET/CT versus mpMRI for the detection of clinically significant prostate cancer: an updated overview. *Semin. Nucl. Med.* **54** (1), 30–38. https://doi.org/10.1053/j.semnuclmed.2023.10.002 (2024).
21. Xiang, M. et al. Performance of a prostate-specific membrane antigen positron emission tomography/computed tomography-derived risk-stratification tool for high-risk and very high-risk prostate cancer. *JAMA Netw. Open.* **4** (12), e2138550. https://doi.org/10.1001/jamanetworkopen.2021.38550 (2021).
22. Cheng, C. et al. Prediction of clinically significant prostate cancer using a novel 68Ga-PSMA PET-CT and multiparametric MRI-based model. *Transl. Androl. Urol.* **12** (7), 1115–1126. https://doi.org/10.21037/tau-22-832 (2023).
23. Tayara, O. M. et al. Comparison of multiparametric MRI, [68Ga]Ga-PSMA-11 PET-CT, and clinical nomograms for primary T and N staging of intermediate-to-high-risk prostate cancer. *Cancers (Basel)* **15** (24), 5838. https://doi.org/10.3390/cancers15245838 (2023).
24. Xing, N. Z. et al. Feasibility of prostatectomy without prostate biopsy in the era of new imaging technology and minimally invasive techniques. *World J. Clin. Cases* **7** (12), 1403–1409. https://doi.org/10.12998/wjcc.v7.i12.1403 (2023).
25. Chaloupka, M. et al. Radical prostatectomy without prior biopsy in patients with high suspicion of prostate cancer based on multiparametric magnetic resonance imaging and prostate-specific membrane antigen positron emission tomography: a prospective cohort study. *Cancers (Basel)* **15** (4), 1266. https://doi.org/10.3390/cancers15041266 (2023).
26. Falkenbach, F. et al. PSA-density, DRE, and PI-RADS 5: potential surrogates for omitting biopsy? *World J. Urol.* **42** (1), 182. https://doi.org/10.1007/s00345-024-04894-6 (2024).
27. Sharma, A. P. et al. Accuracy of combined multi-parametric MRI and PSMA PET-CT in diagnosing localized prostate cancer: newer horizons for a biopsy-free pathway. *Eur. J. Hybrid. Imaging* **7** (1), 24. https://doi.org/10.1186/s41824-023-00182-5 (2023).

Author contributions

X. Jiang designed the study and wrote the main manuscript text; J. Wang, M. Chen, S. Guo, and L. Liu assisted with data analysis and mauscript preparation, data collection and analysis; Y. Xu and L. Liu reviewed the mauscript. All authors contributed to the article and approved the submitted version.

Funding

Dr. Xingkang Jiang reports support from the Tianjin Health Science and Technology Project (No. KJ20169), the Second Hospital of Tianjin Medical University (No. MNRC202312 and No. MYSRC202306). The remaining authors have nothing to disclose.

Declarations

Competing interests
The authors declare no competing interests.

Ethics statement
The present study protocol was reviewed and approved by the institutional review board of the Second Hospital of Tianjin Medical University Hospital (No.KY2020K130). Informed consent was submitted by all subjects when they were enrolled.

Research involving human participants
Institutional Review Board approval was obtained (No.KY2020K130).

Additional information
Supplementary Information The online version contains supplementary material available at https://doi.org/10.1038/s41598-025-86607-6.

Correspondence and requests for materials should be addressed to L.L. or X.J.

Reprints and permissions information is available at www.nature.com/reprints.

Publisher's note Springer Nature remains neutral with regard to jurisdictional claims in published maps and institutional affiliations.

Open Access This article is licensed under a Creative Commons Attribution-NonCommercial-NoDerivatives 4.0 International License, which permits any non-commercial use, sharing, distribution and reproduction in any medium or format, as long as you give appropriate credit to the original author(s) and the source, provide a link to the Creative Commons licence, and indicate if you modified the licensed material. You do not have permission under this licence to share adapted material derived from this article or parts of it. The images or other third party material in this article are included in the article's Creative Commons licence, unless indicated otherwise in a credit line to the material. If material is not included in the article's Creative Commons licence and your intended use is not permitted by statutory regulation or exceeds the permitted use, you will need to obtain permission directly from the copyright holder. To view a copy of this licence, visit http://creativecommons.org/licenses/by-nc-nd/4.0/.

© The Author(s) 2025